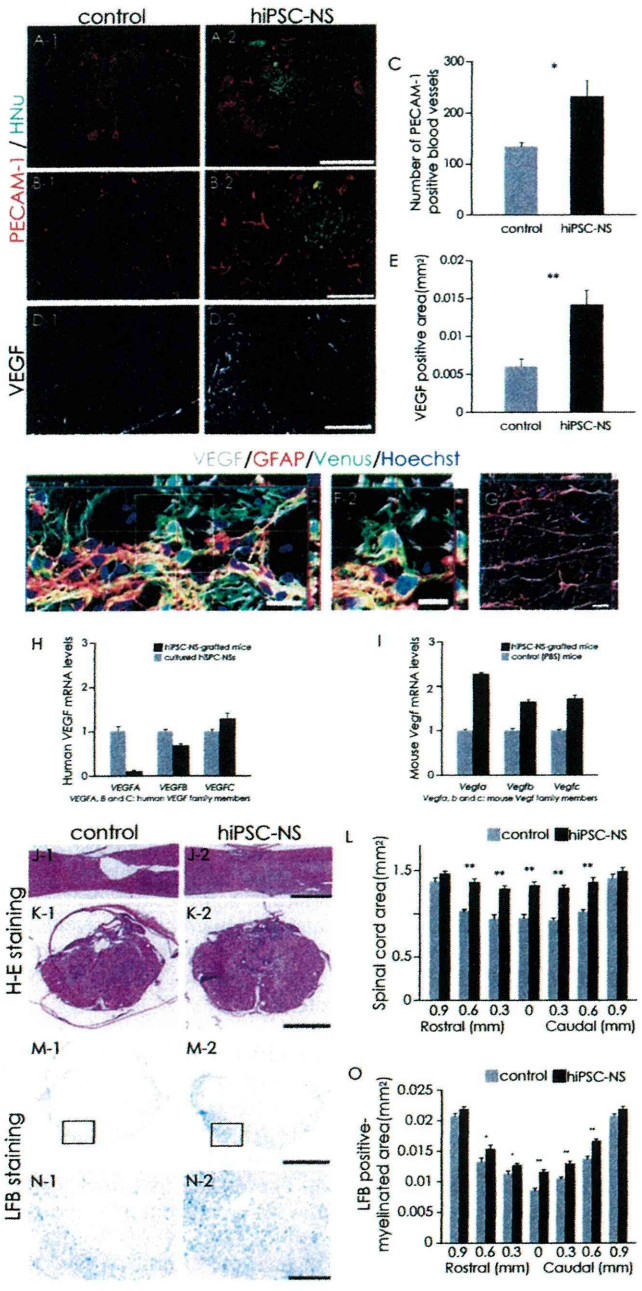

Fig. 3. Transplanted hiPSC-NSs enhanced angiogenesis and prevented atrophic changes and demyelination after SCI. (*A* and *B*) Representative images of PECAM-1$^+$ blood vessels. (*C*) Quantitative analysis of PECAM-1$^+$ blood vessels at the lesion epicenter. Values are means ± SEM (n = 4). (*D*) Representative images of axial sections stained for VEGF. (*E*) Quantitative analysis of the VEGF$^+$ area at the lesion epicenter. Values are means ± SEM (n = 4). (*F* and *G*) Expression of VEGF in GFAP$^+$ astrocytes among Venus$^+$-graft–derived human cells (yellow indicates VEGF$^+$, GFAP$^+$, and Venus$^+$ cells) (*F*) and host mouse-derived cells (*G*) in the spinal cord. (*H*) Expression of human *VEGF* mRNA (*VEGFA*, *-B*, and *-C* are the human *VEGF* family members) 5 d after the hiPSC-NSs were transplanted (black bars) compared with cultured hiPSC-NSs before transplantation (gray bars). Values are means ± SEM (n = 3, each). Human *VEGF* expression was undetectable in the spinal cord of mice treated with PBS. (*I*) Expression of mouse *Vegf* mRNA (*Vegfa*, *-b*, and *-c* are the mouse *Vegf* family members) 5 d after hiPSC-NS transplantation (black bars) or PBS injection (gray bars) into the spinal cord. The mouse *Vegf* expression level was higher in the hiPSC-NS–grafted mice than in PBS-injected mice. Values are means ± SEM (n = 3, each). (*J* and *K*) Representative H&E-stained images of sagittal and axial sections at the lesion epicenter 56 d after SCI. (*L*) Quantitative analysis of the spinal cord area measured in H&E-stained axial sections at different regions. Values are means ± SEM (n = 6). (*M* and *N*) Representative LFB-stained images of the axial sections at the lesion epicenter 56 d after SCI. (*O*) Quantitative analysis of the myelinated area by LFB-stained axial sections at different regions. Values are means ± SEM (n = 6). *P < 0.05, **P < 0.01. (Scale bars, 500 μm in *A*, *K*, and *M*; 200 μm in *B*; 100 μm in *D* and *N*; 20 μm in *F-1* and *G*; 10 μm in *F-2*; and 1,000 μm in *J*.)

a greater preservation of myelinated areas in the hiPSC-NS group compared with the control group (Fig. 3 *M–O*).

To evaluate the effects of hiPSC-NS transplantation on axonal regrowth after SCI, we examined the expression of neurofilament 200 kDa (NF-H), 5-hydroxytrytamine (5HT), and growth-associated protein 43 (GAP43) in the injured spinal cord by immunohistochemistry. There were significantly more NF-H$^+$ neuronal fibers in the hiPSC-NS group than in the control group (Fig. 4 *A* and *B*). 5HT$^+$ fibers, descending serotonergic raphespinal tract axons that are important for the motor functional recovery of hind limbs (20–22), were observed at the lumbar intumescence in all mice (Fig. 4*C*). Contusive SCI resulted in a significant decrease in the number of 5HT$^+$ fibers. Relative to mice at 7 d after SCI (2 d before the transplantation), by 56 d after SCI a slight but significant increase in the 5HT$^+$ fiber area was seen in the control group, and the hiPSC-NS group showed an even greater enhancement (Fig. 4 *C* and *D*).

GAP43$^+$ axons, which are regrowing (23), were detected in the distal cords of all mice, but in the hiPSC-NS group, there were significantly more GAP43$^+$ fibers in the ventral region 1 mm caudal to the lesion epicenter (Fig. 4 *E* and *F*), suggesting that the hiPSC-NS transplantation promoted axonal regrowth in the injured spinal cord. We also observed hiPSC-NS–derived astrocytes closely associated with NF-H$^+$ fibers and 5HT$^+$ fibers (Fig. 4 *G* and *H*). Moreover, RT-PCR revealed the expression of neurotrophic factors (NGF, BDNF, and hepatocyte growth factor, HGF), which are associated with the axonal growth and survival of existing neurons, by both the grafted human cells and the host mouse tissues (Fig. 4 *I* and *J*).

To examine the effect of hiPSC-NSs on structural changes in pain afferents entering the dorsal horn of the spinal cord above and below the injured spinal segments, we investigated the distribution of calcitonin gene-related peptide (CGRP$^+$) fibers, which are involved in peripheral and spinal pain mechanisms (6, 24, 25). We quantified the areas of CGRP$^+$ fibers in lamina III, 4 mm rostral and 4 mm caudal to the lesion epicenter. There were no significant differences in the areas of CGRP$^+$ fibers in lamina III between the hiPSC-NS and control groups (Fig. S2 *A–C*).

Transplanted hiPSC-NSs Promoted Motor Functional and Electrophysiological Recovery After SCI. We evaluated the motor functional recovery by BMS score, Rotarod test, and the DigiGait system. The BMS score showed significantly better functional recovery in the hiPSC-NS than the control group 21 d after SCI and thereafter (Fig. 5*A*). In the Rotarod test, the hiPSC-NS group showed a significantly longer running time than the control group 56 d post-SCI (Fig. 5*B*). The DigiGait system measures the treadmill gait, as an objective evaluation of motor function (26, 27). Whereas all of the hiPSC-NS–grafted mice (n = 18) could walk on the treadmill at 8 cm/s, a subset of the control mice (4 out of 16) could not maintain this speed. The profile of stride length at 8 cm/s clearly demonstrated a significantly better recovery of motor function in the hiPSC-NS–grafted mice compared with the 12 control mice that could walk at this speed (Fig. 5*C*).

Motor-evoked potential (MEP) was used to measure the functional recovery in all of the mice electrophysiologically. The latency of the motor-evoked potential was also measured, from the onset of stimulus to the first response of each wave. At 112 d after SCI, waves were detected in most of the hiPSC-NS group (14 of 17 mice), but none were detected in the control group (0 of 15 mice) (Fig. 5*D*). The average signal-to-response latency in the hiPSC-NS group was 4.6 ± 0.1 ms. Consistent with the

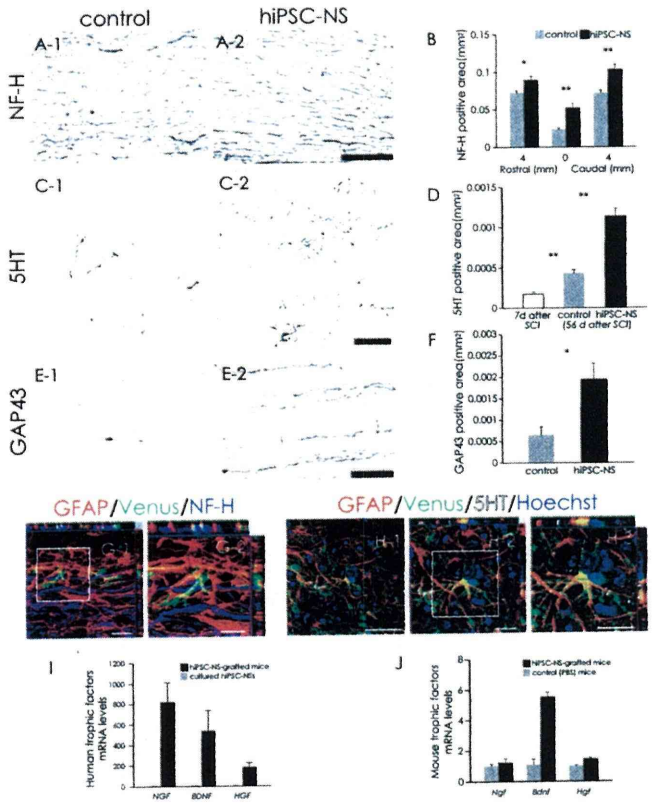

Fig. 4. Transplanted hiPSC-NSs enhanced axonal growth after SCI. (*A*) Representative images of sagittal sections stained for NF-H at the lesion epicenter. (*B*) Quantitative analysis of the NF-H$^+$ area. Values are means ± SEM (n = 4). (*C*) Representative images of axial sections stained for 5HT at the lumbar intumescence. (*D*) Quantitative analysis of the 5HT$^+$ area at the lumbar intumescence in axial sections. Values are means ± SEM (n = 6 each in the 7 d and control 56 d after SCI groups, and n = 5 in the hiPSC-NS (56 d after SCI) group). (*E*) Representative images of midsagittal sections stained for GAP43 in the ventral region 1 mm caudal to the lesion epicenter. (*F*) Quantitative analysis of the GAP43$^+$ area in midsagittal sections. Values are means ± SEM (n = 4). (*G* and *H*) NF-H$^+$ neural fibers and 5HT$^+$ (serotonergic) fibers extended in association with GFAP$^+$/Venus$^+$-graft–derived human astrocytes. (*I*) Expression of human neurotrophic factor mRNAs (*NGF*, *BDNF*, and *HGF*) 5 d after hiPSC-NS transplantation (black bars) compared with cultured hiPSC-NSs before transplantation (gray bars). Values are means ± SEM (n = 3, each). (*J*) Expression of mouse neurotrophic factor mRNAs (*Ngf*, *Bdnf*, and *Hgf*) 5 d after hiPSC-NS transplantation (black bars) or PBS injection (gray bars) into the spinal cord. Values are means ± SEM (n = 3, each). *P < 0.05, **P < 0.01. (Scale bars, 100 μm in *A*; 50 μm in *C*, *E*, and *H-1*; 20 μm in *G-1*, *H-2*, and *H-3*; and 10 μm in *G-2*.)

electrophysiology results, α-CaM kinase 2$^+$ descending motor axons were observed to persist in the lesion epicenter in the hiPSC-NS group (Fig. S3).

Long-Term Observation Revealed No Tumor Formation After hiPSC-NS Transplantation. To investigate the long-term safety of the grafted hiPSC-NSs, we extended the follow-up period to 112 d after SCI. Motor functional recovery was maintained in the hiPSC-NS group for the entire period (Fig. 6*A*), the hiPSC-NS–grafted mice showed no tumor formation (Fig. 6*B*), and the grafted cells exhibited normal neural differentiation (Fig. 6*C*). We determined the proportion of Venus$^+$ grafted cells that were immunopositive for each cell-type–specific marker 112 d after SCI. The grafted hiPSC-NSs had differentiated into NeuN$^+$ (40.2 ± 2.8%), βIII tubulin$^+$ (50.7 ± 2.0%), GFAP$^+$ (18.1 ± 2.2%), APC$^+$ (8.9 ± 1.6%), and Nestin$^+$ (7.5 ± 1.0%) cells. For comparison, at 56 d after SCI, the grafted cells had differentiated

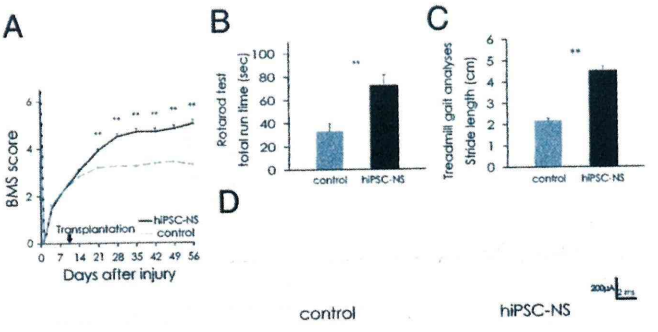

Fig. 5. Transplanted hiPSC-NSs promoted motor functional and electrophysiological recovery after SCI. (*A*) Motor function in the hindlimbs was assessed weekly by the BMS score for 56 d. Values are means ± SEM. (*B*) Rotarod test 56 d after SCI. Graph shows the total run time. Values are means ± SEM. (*C*) Treadmill gait analysis using the DigiGait system 56 d after SCI. Graph shows stride length. Values are means ± SEM. (*D*) Electrophysiological analysis performed 112 d after SCI. MEP waves were detected in most of the hiPSC-NS group (14 out of 17), whereas they were not detected in the control group (0 out of 15). **P < 0.01. Behavioral analyses were assessed by two observers who were blind to the treatment.

into NeuN$^+$ (22.9 ± 1.0%), βIII tubulin$^+$ (49.1 ± 2.0%), GFAP$^+$ (17.0 ± 1.2%), APC$^+$ (3.0 ± 0.4%), and Nestin$^+$ (10.7 ± 2.2%) cells (Fig. 6*D*). Notably, significantly higher percentages of NeuN$^+$ mature neurons and APC$^+$ oligodendrocytes were present at 112 d than at 56 d after SCI, whereas the percentage of graft-derived human Nestin$^+$ NS/PCs slightly decreased. We also examined the amount of proliferation among the grafted cells by K_i-67 labeling. The percentage of K_i-67$^+$/HNu$^+$ cells was significantly decreased between 56 d post-SCI (1.1 ± 0.2%) and 112 d post-SCI (0.7 ± 0.1%). The K_i-67$^+$/HNu$^+$ cells were dispersed throughout the graft area without evidence of clustering at particular sites.

Discussion

In the present study, we used clone 201B7 of hiPSC-derived neurospheres as a cell source to treat SCI in adult NOD-SCID mice. We demonstrated that the hiPSC-NSs differentiated into neurons, astrocytes, and oligodendrocytes in the injured spinal cord and promoted motor functional recovery. Hypothetically, the transplantation of hiPSC-NSs could result in a wide range of positive effects, including angiogenesis, axonal regeneration, and local-circuitry reconstruction, which have been reported in previous studies using rodent ESCs or iPSCs for SCI treatment (12, 18). All these mechanisms could contribute to motor functional recovery after hiPSC-NS transplantation for SCI.

Angiogenesis after SCI promotes endogenous repair and supports axonal outgrowth (28, 29). Here we observed that the transplantation of hiPSC-NSs enhanced angiogenesis and tissue sparing after SCI. Astrocytes express angiogenic growth factors such as VEGF under hypoxic conditions (12, 30, 31), and we observed that the hiPSC-derived astrocytes and host astrocytes expressed VEGF, suggesting that the transplantation of hiPSC-NSs promoted VEGF expression in both host- and graft-derived astrocytes.

Motor functional recovery was also supported by the axonal regrowth that was promoted by the transplanted hiPSC-NSs. Our immunohistochemical analyses revealed grafted hiPSC-derived GFAP$^+$ astrocytes closely associated with NF-H$^+$ and 5HT$^+$ fibers. Graft-derived astrocytes are reported to promote the regrowth of NF-H$^+$ and 5HT$^+$ fibers by offering a growth-permissive substrate (12, 18, 32). Furthermore, neurotrophic factors such as NGF, BDNF, and HGF play critical roles in axonal growth and in the survival of existing neurons (33–38). Consistent with these reports, we observed that hiPSC-NS transplantation promoted axonal regrowth at the distal spinal cord. Because our treatment induced axonal regrowth, we also exam-

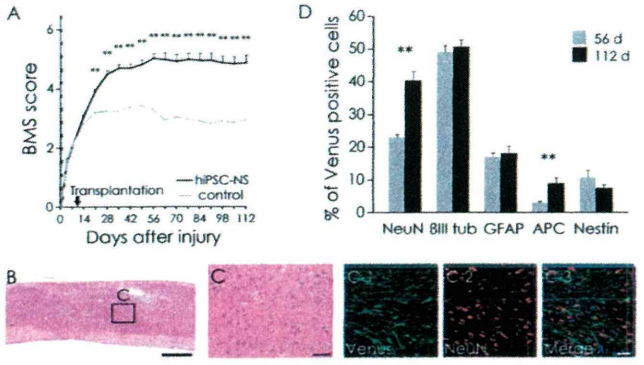

Fig. 6. Long-term observation revealed no tumor formation after hiPSC-NS transplantation. (*A*) For 112 d, motor function in the hindlimbs was assessed weekly by the BMS score. Values are means ± SEM. (*B*) Representative H&E image of hiPSC-NS–grafted mice. (*C*) Boxed area in *B*. (*C-1–C-3*) Immunohistochemistry showing normal neural differentiation of the grafted cells. (*D*) Percentages of cell-type–specific marker-positive cells among the Venus$^+$ human cells 56 and 112 d after SCI. Values are means ± SEM (n = 4 and 5, respectively). $^{**}P < 0.01$. (Scale bars, 500 μm in *B*; and 50 μm in *C*.)

ined the pain afferents entering lamina III of the spinal cord, which is closely associated with NS/PC-transplantation–induced allodynia (6). Our analysis revealed no significant differences between the hiPSC-NS and control groups. Thus, although allodynia was not assessed, our morphological data suggested that hiPSC-NS transplantation did not induce abnormal innervation by pain afferents, in contrast to a previous study in which NS/PCs derived from adult rat spinal cord were transplanted into a rat SCI model (6).

The motor functional recovery observed in this study may also be due to the formation of synapses between hiPSC-derived neurons and host mouse spinal cord neurons. Our present data support the potential for grafted hiPSC-NSs to form synapses with host neurons in the injured spinal cord. Previous studies have shown post-SCI functional improvements associated with intraspinal grafts containing neuronal progenitors either alone or in combination with other cells or interventions (4, 7, 39–43). Such studies also report that graft-derived human neurons can receive projections from host mouse neurons and that their extended processes make synapses with host neurons (39). It is likely that local neurons in the lesioned area (a mixture of preserved host neurons and graft-derived neurons) transmit signals by relay.

We observed that most of the hiPSC-derived mature neurons were GABAergic, a neurotransmitter type that plays important roles in the spinal cord by controlling the levels of motoneuronal output and sensory input, by modulating primary afferent transmitter release, and by direct postsynaptic inhibition of motoneurons (44, 45). Furthermore, hypofunctioning spinal GABAergic inhibition is involved in pathological pain states that develop due to SCI (46). Thus, synapse formation by donor-derived GABAergic neurons might be important for motor coordination within the spinal neuronal network and for the suppression of SCI-induced spasticity (8, 47) and pain (46).

The greatest potential drawback of hiPSC-based therapies is their potential for tumorigenicity. Therefore, we observed the treated animals for an extended period. Not only was functional recovery maintained in the hiPSC-NS group for 112 d after SCI, but no tumor formation occurred at all. Quantitative analysis of the phenotype of the grafted hiPSC-NSs revealed an increase in the percentages of NeuN$^+$ mature neurons and APC$^+$ oligodendrocytes at 112 d compared with 56 d after SCI, showing that most of the grafted hiPSC-NSs successfully differentiated into mature neural cells over time. Some Nestin$^+$/HNu$^+$ cells and K_i-67$^+$/HNu$^+$ cells were still present at 112 d post-SCI, although their proportions were lower than at 56 d after SCI, indicating that some grafted cells remained as NS/PCs. However, no evidence of excessive proliferation, clusters of proliferating cells, or other signs of tumor formation were observed in any of the transplant-receiving mice. Collectively, the lack of tumors, increase in NeuN numbers over time, and low Nestin and K_i-67 numbers support the possibility that this approach will be safe in humans.

Consistent with our findings, previous studies using human fetal NS/PCs showed some Nestin$^+$/HNu$^+$ cells that were negative for the proliferative markers K_i-67 and proliferating cell nuclear antigen in the striatum of NOD-SCID mice, 6 mo after transplantation (48), 28–34% Nestin$^+$/HNu$^+$, and 2–4% K_i-67$^+$/HNu$^+$ cells were in the spinal cord of NOD-SCID mice 4 mo after transplantation (5), and 11–14% Nestin$^+$/HNu$^+$ and 3–5% K_i-67$^+$/HNu$^+$ cells were in the spinal cord of nude rats 6 mo after transplantation (49). Notably, no tumor formation was observed in any of these studies, despite the presence of Nestin$^+$- and K_i-67$^+$–grafted cells, even after long-term observation.

Recently, clinical trials of human stem-cell–based therapy for SCI have been launched, using human NS/PCs (4, 5) or human ESC-derived OPCs (15). In this paradigm, OPC-mediated restoration of myelination and trophic effects are the most likely mechanisms for the resulting benefits. Besides overcoming concerns about immune responses and the ethics of using human ESCs (hESCs), our present study suggests that grafted hiPSC-NSs might be more beneficial than hESCs, because the hiPSC-NSs gave rise to GABAergic neurons, which can help to suppress SCI-induced spasticity and pain (8, 46, 47). In addition, we found that hiPSC-NSs differentiated into astrocytes and oligodendrocytes, which can exert positive effects through both cell-autonomous and noncell-autonomous (trophic) mechanisms. Nevertheless, our present results are only a first step toward clinical applications. In our future studies, the safety and effectiveness of hiPSC-derived NS/PCs will be more intensively investigated, for example, using nonhuman primate SCI models (8). In particular, hiPSCs established by delivering the reprogramming factors using a different method, such as an integration-free virus system (50), or a virus-free (51) or transgene-free system (52–54), or by using (HLA)-homozygous donor-derived cells (55), should be evaluated.

Materials and Methods

Cell Culture, Neural Induction, and Lentivirus Transduction. The cell culture and neural induction of hiPSCs (201B7) were performed as described previously (11, 18, 56) with slight modifications.

Lentivirus was prepared and transduced into neurospheres as described previously (11). Briefly, hiPSC-derived primary neurospheres were dissociated and infected with lentivirus expressing Venus fluorescent protein under control of the EF promoter (pCSII-EF–Venus). These primary neurospheres were passaged into secondary and tertiary neurospheres and used for transplantation.

Spinal Cord Injury Model and Transplantation. Adult female NOD-SCID mice (20–22 g) were anesthetized via an i.p. injection of ketamine (100 mg/kg) and xylazine (10 mg/kg). Contusive SCI was induced at the Th10 level using an IH impactor (60 kdyn; Precision Systems and Instrumentation), as described previously (57).

Nine days after the injury, 5×10^5 hiPSC-NSs were transplanted into the lesion epicenter of each mouse (n = 31) using a glass micropipette and stereotaxic injector (KDS310; Muromachi-Kikai). An equal volume of PBS was injected instead into control mice (n = 29).

Behavioral and Histological Analyses. Behavioral analyses were evaluated using the BMS, Rotarod apparatus (Muromachi Kikai), and the DigiGait system (Mouse Specifics) (detailed protocols are described in *SI Materials and Methods*). For histological analyses, mice were deeply anesthetized and intracardially perfused with 4% paraformaldehyde (PFA; pH 7.4). The dissected spinal cords were then sectioned into axial/sagittal sections using a cryostat (detailed conditions are in *SI Materials and Methods*). All behavioral and histological analyses were conducted by observers blind to the treatment. All animal experiments were approved by the ethics committee

of Keio University and were in accordance with the Guide for the Care and Use of Laboratory Animals (National Institutes of Health, Bethesda, MD).

ACKNOWLEDGMENTS. We thank Drs. K. Kitamura, N. Nagoshi, M. Mukaino, A. Iwanami, F. Renault-Mihara, S. Shibata, H. Shimada, T. Harada, S. Miyao, and H.J. Okano for technical assistance and scientific discussions; S. Kaneko for critical proofreading of the manuscript; and all the members of the H.O. and S.Y. laboratories for encouragement and generous support. We also thank Dr. K. Takahashi for the undifferentiated iPS cells. This work was supported by grants from Grants-in-Aid for Scientific Research from Japan Society for the Promotion of Science (SPS) and the Ministry of Education, Culture, Sports, Science, and Technology of Japan (MEXT); the Project for Realization of Regenerative Medicine; and Support for Core Institutes for iPS Cell Research from the MEXT; Japan Science and Technology–California Institute for Regenerative Medicine collaborative program; the Kanrinmaru project from Keio University; Research Fellowships for Young Scientists from JSPS; Keio Gijuku Academic Development Funds; by a Grant-in-Aid for the Global COE program from MEXT to Keio University; and by a Grant-in-Aid for Scientific Research on Innovative Areas (Comprehensive Brain Science Network) from the Ministry of Education, Science, Sports and Culture of Japan.

1. Björklund A, Lindvall O (2000) Cell replacement therapies for central nervous system disorders. *Nat Neurosci* 3:537–544.
2. Gage FH (2000) Mammalian neural stem cells. *Science* 287:1433–1438.
3. Lindvall O, Kokaia Z (2006) Stem cells for the treatment of neurological disorders. *Nature* 441:1094–1096.
4. Cummings BJ, et al. (2005) Human neural stem cells differentiate and promote locomotor recovery in spinal cord-injured mice. *Proc Natl Acad Sci USA* 102: 14069–14074.
5. Salazar DL, Uchida N, Hamers FP, Cummings BJ, Anderson AJ (2010) Human neural stem cells differentiate and promote locomotor recovery in an early chronic spinal cord injury NOD-scid mouse model. *PLoS ONE* 5:e12272.
6. Hofstetter CP, et al. (2005) Allodynia limits the usefulness of intraspinal neural stem cell grafts; directed differentiation improves outcome. *Nat Neurosci* 8:346–353.
7. Ogawa Y, et al. (2002) Transplantation of in vitro-expanded fetal neural progenitor cells results in neurogenesis and functional recovery after spinal cord contusion injury in adult rats. *J Neurosci Res* 69:925–933.
8. Iwanami A, et al. (2005) Transplantation of human neural stem cells for spinal cord injury in primates. *J Neurosci Res* 80:182–190.
9. Okada S, et al. (2005) In vivo imaging of engrafted neural stem cells: Its application in evaluating the optimal timing of transplantation for spinal cord injury. *FASEB J* 19: 1839–1841.
10. Okada Y, Shimazaki T, Sobue G, Okano H (2004) Retinoic-acid-concentration-dependent acquisition of neural cell identity during in vitro differentiation of mouse embryonic stem cells. *Dev Biol* 275:124–142.
11. Okada Y, et al. (2008) Spatiotemporal recapitulation of central nervous system development by murine embryonic stem cell-derived neural stem/progenitor cells. *Stem Cells* 26:3086–3098.
12. Kumagai G, et al. (2009) Roles of ES cell-derived gliogenic neural stem/progenitor cells in functional recovery after spinal cord injury. *PLoS ONE* 4:e7706.
13. Keirstead HS, et al. (2005) Human embryonic stem cell-derived oligodendrocyte progenitor cell transplants remyelinate and restore locomotion after spinal cord injury. *J Neurosci* 25:4694–4705.
14. Sharp J, Frame J, Siegenthaler M, Nistor G, Keirstead HS (2010) Human embryonic stem cell-derived oligodendrocyte progenitor cell transplants improve recovery after cervical spinal cord injury. *Stem Cells* 28:152–163.
15. Strauss S (2010) Geron trial resumes, but standards for stem cell trials remain elusive. *Nat Biotechnol* 28:989–990.
16. Takahashi K, Yamanaka S (2006) Induction of pluripotent stem cells from mouse embryonic and adult fibroblast cultures by defined factors. *Cell* 126:663–676.
17. Okita K, Ichisaka T, Yamanaka S (2007) Generation of germline-competent induced pluripotent stem cells. *Nature* 448:313–317.
18. Tsuji O, et al. (2010) Therapeutic potential of appropriately evaluated safe-induced pluripotent stem cells for spinal cord injury. *Proc Natl Acad Sci USA* 107:12704–12709.
19. Takahashi K, et al. (2007) Induction of pluripotent stem cells from adult human fibroblasts by defined factors. *Cell* 131:861–872.
20. Bregman BS (1987) Spinal cord transplants permit the growth of serotonergic axons across the site of neonatal spinal cord transection. *Brain Res* 431:265–279.
21. Saruhashi Y, Young W, Perkins R (1996) The recovery of 5-HT immunoreactivity in lumbosacral spinal cord and locomotor function after thoracic hemisection. *Exp Neurol* 139:203–213.
22. Kim D, et al. (1999) Direct agonists for serotonin receptors enhance locomotor function in rats that received neural transplants after neonatal spinal transection. *J Neurosci* 19:6213–6224.
23. Kobayashi NR, et al. (1997) BDNF and NT-4/5 prevent atrophy of rat rubrospinal neurons after cervical axotomy, stimulate GAP-43 and Talpha1-tubulin mRNA expression, and promote axonal regeneration. *J Neurosci* 17:9583–9595.
24. Krenz NR, Weaver LC (1998) Sprouting of primary afferent fibers after spinal cord transection in the rat. *Neuroscience* 85:443–458.
25. Krenz NR, Meakin SO, Krassioukov AV, Weaver LC (1999) Neutralizing intraspinal nerve growth factor blocks autonomic dysreflexia caused by spinal cord injury. *J Neurosci* 19:7405–7414.
26. Li S, Kim JE, Budel S, Hampton TG, Strittmatter SM (2005) Transgenic inhibition of Nogo-66 receptor function allows axonal sprouting and improved locomotion after spinal injury. *Mol Cell Neurosci* 29:26–39.
27. Springer JE, et al. (2010) The functional and neuroprotective actions of Neu2000, a dual-acting pharmacological agent, in the treatment of acute spinal cord injury. *J Neurotrauma* 27:139–149.
28. Beattie MS, et al. (1997) Endogenous repair after spinal cord contusion injuries in the rat. *Exp Neurol* 148:453–463.
29. Kim HM, Hwang DH, Lee JE, Kim SU, Kim BG (2009) Ex vivo VEGF delivery by neural stem cells enhances proliferation of glial progenitors, angiogenesis, and tissue sparing after spinal cord injury. *PLoS ONE* 4:e4987.
30. Yoshida H, et al. (2002) Platelet-activating factor enhances the expression of vascular endothelial growth factor in normal human astrocytes. *Brain Res* 944:65–72.
31. Mense SM, et al. (2006) Gene expression profiling reveals the profound upregulation of hypoxia-responsive genes in primary human astrocytes. *Physiol Genomics* 25: 435–449.
32. Hofstetter CP, et al. (2002) Marrow stromal cells form guiding strands in the injured spinal cord and promote recovery. *Proc Natl Acad Sci USA* 99:2199–2204.
33. Jones LL, Oudega M, Bunge MB, Tuszynski MH (2001) Neurotrophic factors, cellular bridges and gene therapy for spinal cord injury. *J Physiol* 533:83–89.
34. Brock JH, et al. (2010) Local and remote growth factor effects after primate spinal cord injury. *J Neurosci* 30:9728–9737.
35. Jakeman LB, Wei P, Guan Z, Stokes BT (1998) Brain-derived neurotrophic factor stimulates hindlimb stepping and sprouting of cholinergic fibers after spinal cord injury. *Exp Neurol* 154:170–184.
36. Tuszynski MH, et al. (1996) Nerve growth factor delivery by gene transfer induces differential outgrowth of sensory, motor, and noradrenergic neurites after adult spinal cord injury. *Exp Neurol* 137:157–173.
37. Tuszynski MH (1997) Gene therapy for nervous system disease. *Ann N Y Acad Sci* 835: 1–11.
38. Kitamura K, et al. (2007) Hepatocyte growth factor promotes endogenous repair and functional recovery after spinal cord injury. *J Neurosci Res* 85:2332–2342.
39. Abematsu M, et al. (2010) Neurons derived from transplanted neural stem cells restore disrupted neuronal circuitry in a mouse model of spinal cord injury. *J Clin Invest* 120:3255–3266.
40. Mitsui T, Shumsky JS, Lepore AC, Murray M, Fischer I (2005) Transplantation of neuronal and glial restricted precursors into contused spinal cord improves bladder and motor functions, decreases thermal hypersensitivity, and modifies intraspinal circuitry. *J Neurosci* 25:9624–9636.
41. Kim BG, Dai HN, Lynskey JV, McAtee M, Bregman BS (2006) Degradation of chondroitin sulfate proteoglycans potentiates transplant-mediated axonal remodeling and functional recovery after spinal cord injury in adult rats. *J Comp Neurol* 497: 182–198.
42. White TE, et al. (2010) Neuronal progenitor transplantation and respiratory outcomes following upper cervical spinal cord injury in adult rats. *Exp Neurol* 225:231–236.
43. Bonner JF, Blesch A, Neuhuber B, Fischer I (2010) Promoting directional axon growth from neural progenitors grafted into the injured spinal cord. *J Neurosci Res* 88: 1182–1192.
44. Schneider SP, Fyffe RE (1992) Involvement of GABA and glycine in recurrent inhibition of spinal motoneurons. *J Neurophysiol* 68:397–406.
45. Malcangio M, Bowery NG (1996) GABA and its receptors in the spinal cord. *Trends Pharmacol Sci* 17:457–462.
46. Kim DS, et al. (2010) Transplantation of gabaergic neurons from ES cells attenuates tactile hypersensitivity following spinal cord injury. *Stem Cells* 28:2099–2108.
47. Watanabe K, et al. (2004) Comparison between fetal spinal-cord- and forebrain-derived neural stem/progenitor cells as a source of transplantation for spinal cord injury. *Dev Neurosci* 26:275–287.
48. Ogawa D, et al. (2009) Evaluation of human fetal neural stem/progenitor cells as a source for cell replacement therapy for neurological disorders: Properties and tumorigenicity after long-term in vitro maintenance. *J Neurosci Res* 87:307–317.
49. Yan J, et al. (2007) Extensive neuronal differentiation of human neural stem cell grafts in adult rat spinal cord. *PLoS Med* 4:e39.
50. Fusaki N, Ban H, Nishiyama A, Saeki K, Hasegawa M (2009) Efficient induction of transgene-free human pluripotent stem cells using a vector based on Sendai virus, an RNA virus that does not integrate into the host genome. *Proc Jpn Acad, Ser B, Phys Biol Sci* 85:348–362.
51. Okita K, Nakagawa M, Hyenjong H, Ichisaka T, Yamanaka S (2008) Generation of mouse induced pluripotent stem cells without viral vectors. *Science* 322:949–953.
52. Zhou H, et al. (2009) Generation of induced pluripotent stem cells using recombinant proteins. *Cell Stem Cell* 4:381–384.
53. Warren L, et al. (2010) Highly efficient reprogramming to pluripotency and directed differentiation of human cells with synthetic modified mRNA. *Cell Stem Cell* 7: 618–630.
54. Rhee YH, et al. (2011) Protein-based human iPS cells efficiently generate functional dopamine neurons and can treat a rat model of Parkinson disease. *J Clin Invest* 121: 2326–2335.
55. Okita K, et al. (2011) A more efficient method to generate integration-free human iPS cells. *Nat Methods* 8:409–412.
56. Miura K, et al. (2009) Variation in the safety of induced pluripotent stem cell lines. *Nat Biotechnol* 27:743–745.
57. Scheff SW, Rabchevsky AG, Fugaccia I, Main JA, Lumpp JE, Jr. (2003) Experimental modeling of spinal cord injury: Characterization of a force-defined injury device. *J Neurotrauma* 20:179–193.

Journal of Neuroscience Research

Journal of Neuroscience Research 89:86–95 (2011)

Strong Neurogenesis, Angiogenesis, Synaptogenesis, and Antifibrosis of Hepatocyte Growth Factor in Rats Brain After Transient Middle Cerebral Artery Occlusion

Jingwei Shang,[1] Kentaro Deguchi,[1] Yasuyuki Ohta,[1] Ning Liu,[1] Xuemei Zhang,[1] Fengfeng Tian,[1] Toru Yamashita,[1] Yoshio Ikeda,[1] Tohru Matsuura,[1] Hiroshi Funakoshi,[2] Toshikazu Nakamura,[3] and Koji Abe[1]*

[1]Department of Neurology, Okayama University Graduate School of Medicine, Dentistry and Pharmaceutical Sciences, Okayama, Japan
[2]Division of Molecular Regenerative Medicine, Department of Biochemistry and Molecular Biology, Osaka University Graduate School of Medicine, Osaka, Japan
[3]Kringle Pharma Joint Research Division for Regenerative Drug Discovery, Center for Advanced Medicine, Osaka University, Osaka, Japan

Hepatocyte growth factor (HGF) and glial cell line-derived neurotrophic factor (GDNF) are strong neurotrophic factors. However, their potentials in neurogenesis, angiogenesis, synaptogenesis, and antifibrosis have not been compared. Therefore, we investigated these effects of HGF and GDNF in cerebral ischemia in the rat. Wistar rats were subjected to 90 min of transient middle cerebral artery occlusion (tMCAO). Immediately after reperfusion, HGF or GDNF was given by topical application. BrdU was injected intraperitoneally twice daily 1, 2, and 3 days after tMCAO. On 14 day, we histologically evaluated infarct volume, antiapoptotic effect, neurogenesis, angiogenesis, synaptogenesis, and antifibrosis. Both HGF and GDNF significantly reduced infarct size and the number of TUNEL-positive cells, but only HGF significantly increased the number of BrdU-positive cells in the subventricular zone, and 5′-bromo-2′-deoxyuridine -positive cells differentiated into mature neurons on the ischemic side. Enhancement of angiogenesis and synaptogenesis at the ischemic boundary zone was also observed only in HGF-treated rats. HGF significantly decreased the glial scar formation and scar thickness of the brain pia mater after tMCAO, but GDNF did not. Our study shows that both HGF and GDNF had significant neurotrophic effects, but only HGF can promote the neurogenesis, angiogenesis, and synaptogenesis and inhibit fibrotic change in brains after tMCAO.

Key words: angiogenesis; antifibrosis; cerebral ischemia; neurogenesis; synaptogenesis

The risk of cerebrovascular events is increasing and is becoming important issue. Acute stroke is a major cause of death and disability worldwide, and only a small percentage of hospitalized patients receive therapy. At present, scientists have intensified their work on pharmacological approaches beyond the hyperacute phase of stroke. The time window for therapies improving stroke recovery, called *neurorestorative therapies*, is likely to be far longer than that for acute neuroprotection (Abe, 2000; Chen and Chopp, 2006). Neurorestorative events include neurogenesis, angiogenesis, and synaptic plasticity, all of which contribute to functional improvement after stroke. Neurogenesis, the process through which precursor cells differentiate toward a mature neuronal phenotype, persists in discrete regions of the adult brain, including the rostral subventricular zone (SVZ) and the subgranular zone (SGZ) of the hippocampal dentate gyrus (Kernie and Parent, 2009). Angiogenesis is an important process for forming new brain microvessels after cerebral ischemia, which is essential in reproduction, development, and wound repair (Folkman and Shing, 1992). Synaptic

Contract grant sponsor: Ministry of Education, Science, Culture and Sports of Japan; Contract grant number: 21390267; Contract grant sponsor: Reasearch Committee of CNS Degenerative Diseases (to I. Nakano); Contract grant sponsor: Ministry of Health, Labour and Welfare of Japan (to Y. Itoyama. T. Imai).

*Correspondence to: Koji Abe, Okayama University Graduate School of Medicine, Dentistry and Pharmaceutical Sciences, 2-5-1 Shikatacho, Okayama 700-8558, Japan. E-mail: shangjw@cc.okayama-u.ac.jp

Received 22 July 2010; Revised 29 August 2010; Accepted 30 August 2010

Published online 20 October 2010 in Wiley Online Library (wileyonlinelibrary.com). DOI: 10.1002/jnr.22524

plasticity is related to behavioral change and functional recoveries after brain injury (Nudo, 2003).

Hepatocyte growth factor (HGF) is a multifunctional growth factor originally characterized as a potent mitogen for hepatocytes in primary culture (Nakamura et al., 1989). HGF plays important roles in mitogenesis, motogenesis, morphogenesis, angiogenesis, and antiapoptosis (Nakamura et al., 1989; Zarnegar and Michalopoulos, 1995; Matsumoto and Nakamura, 1996). In the brain, HGF has the functions as a neurotrophic factor and an angiogenic factor (Miyazawa et al., 1998; Van Belle et al., 1998).

Glial cell line-derived neurotrophic factor (GDNF), a member of the transforming growth factor-β superfamily, has a potent neuroprotective effect on a variety of neuronal damage both in vitro and in vivo (Beck et al., 1995; Abe et al., 1997; Yamashita et al., 2009b). Topical application and intracerebral administration of GDNF decreased the size of ischemia-induced brain infarction and the number of TUNEL-positive neurons with suppression of the apoptotic pathways (Abe et al., 1997).

However, the potentials for angiogenesis, neurogenesis, synaptogenesis, and antifibrosis of HGF and GDNF have not been directly compared. Therefore, we investigated HGF and GDNF effects on angiogenesis, neurogenesis, synaptogenesis, and antifibrosis in the postischemic brain.

MATERIALS AND METHODS

Surgical Preparation

Adult male Wistar rats (SLC, Shizuoka, Japan) weighing 250–280 g were used for the experiments. The animals were anesthetized with an intraperitoneal injection of 40 mg/kg pentobarbital and positioned in a stereotaxic operating apparatus. A 2-mm-diameter burr hole was carefully made at 3 mm dorsal and 4 mm lateral to the right from the bregma using an electric dental drill, avoiding traumatic brain injury. Dura mater was preserved at that time. The location of the burr hole was in the upper part of the right middle cerebral artery (MCA) territory. Then, the incision was closed, and the animals were allowed free access to water and food at room temperature. On the next day, at about 24 hr after the drilling, the rats were lightly anesthetized by inhalation of a 69%/30% (v/v) mixture of nitrous oxide/oxygen and 1% halothane using a facemask. A midline neck incision was made, and the right common carotid artery was exposed, and then inhalation of anesthetics was stopped. When the animal began to regain consciousness, the right MCA was occluded for 90 min by insertion of 4-0 surgical nylon thread with silicone coating through the common carotid artery (Abe et al., 1992). With this technique, the tip of the thread occludes the origin of the right MCA. The reliability of producing successful strokes is almost complete in this model (Koizumi et al., 1986). During these procedures, body temperature was monitored with a rectal probe and maintained at 37°C ± 0.3°C using a heating pad. The surgical incision was then closed, and the animals were allowed to recover at room temperature. After 90 min of tMCAO, CBF was restored by removal of the nylon thread.

HGF or GDNF Treatment In Vivo

Just after the restoration of CBF, the dura mater under the burr hole was carefully removed, and a small piece (8 mm^3) of spongel (Yamanouchi Pharma Co.) presoaked in 9 μl Ringer's solution (Otsuka Pharma Co.) as vehicle or a solution containing HGF (30.0 μg in 9 μl of vehicle; Kringle Pharma, Osaka Japan) or GDNF (3.0 μg in 9 μl of vehicle; Sigma, St. Louis, MO) was placed in contact with the surface of the cerebral cortex (Abe et al., 1997). In terms of the dose of HGF, 5.0, 10.0 and 30.0 μg were checked in our preliminary experiment (Miyazawa et al., 1998; Niimura et al., 2006), and the effect of 30.0 μg in 9 μl of vehicle was the best. The dose of GDNF was chosen based on our previous report (Abe et al., 1997). The spongel was buried in the skull bone. The surface of the skull bone was then covered with vinyl tape, and the head skin incision was closed. It is reported that application of growth factor in spongel is as effective as chronic infusion (Otto et al., 1989). These operations were performed in a sterile fashion. Sham-operated control animals underwent burr hole surgery, exposure of the common carotid artery without tMCAO, and placement of spongel presoaked in vehicle. The experimental protocol and procedures were approved by the Animal Committee of Okayama University School of Medicine.

5′-Bromo-2′-Deoxyuridine Labeling

5′-Bromo-2′-deoxyuridine (BrdU; Sigma), a thymidine analog that is incorporated into the DNA of dividing cells during S-phase (Lee et al., 2007), was used to label proliferative cells. It was dissolved in saline and injected intraperitoneally (50 mg/kg) on days 1, 2, and 3 after tMCAO or vehicle operation twice per day (total dose of 300 mg/kg rat; Deguchi et al., 2006).

Tissue Preparation

The animals (n = 5) were sacrificed at day 14 after the restoration of CBF under deep anesthesia with pentobarbital (10 mg/250 g rat). The rats were transcardially perfused with heparinized saline followed by 4% paraformaldehyde in phosphate buffer (PB). The whole brain was subsequently removed and immersed in the same fixation for 12 hr at 4°C. After washing out paraformaldehyde by PB, the brain was immersed in sucrose solution in PB, rapidly frozen in powdered dry ice, and then stored at −80°C. Coronal brain sections of 20 μm thickness were prepared by using a cryostat and mounted on a silane-coated glass.

Infarct Volume Measurement

For quantitative analysis of infarct volume, the sections were stained with hematoxylin and eosin (HE) and observed with a light microscope (Olympus BX-51; Olympus Optical). The area of the infarct was measured in five sections by pixel counting using Photoshop 7.0, and the volume was calculated.

TUNEL Staining

To evaluate antiapoptotic effects, terminal deoxynucleotidyl transferase-mediated dUTP-biotin in situ nick end labeling (TUNEL) study was performed with a kit (Roche, Nonnenwald, Germany), which detects double-strand breaks in genomic DNA with diaminobenzidine in accordance with our previous report (Abe et al., 1997).

Single Immunohistochemical Analysis

We performed immunohistochemistry for BrdU, growth associated protein-43 (GAP-43), and α-smooth muscle actin (α-SMA). BrdU is used to label proliferative cells, and GAP-43 is associated with axon growth and synaptogenesis as well as synaptic remodeling (Oestreicher et al., 1997). After fixation with formaldehyde and endogenous peroxidase activity quenching, sections were incubated with bovine serum albumin for 1 hr. Then, they were incubated with primary antibody for BrdU (1:200; Oncogene Research Products), GAP-43 (1:200; Sigma), and α-SMA (1:200; Sigma) at 4°C overnight. On the next day, we treated the sections with mouse monoclonal biotinylated secondary antibody (1:200; Vector, Burlingame, CA) for 2 hr at room temperature. Immunoreactivities were developed in horseradish peroxidase-streptavidin-biotin complex solution (Vectastain ABC kit; Vector) for 30 min and then incubated with DAB.

Double-Fluorescence Immunohistochemistry

To determine neurogenesis and angiogenesis effects, double- immunofluorescence studies were performed for BrdU plus doublecortin (DCX), glial fibrillary acidic protein (GFAP), and N-acetylglucosamine oligomers (NAGO). *Lycopersicon esculentum* lectin (LEL) is a glycoprotein with affinity for NAGO, which mature vascular endothelial cells express (Augustin et al., 1995), To examine antifibrotic effects, double-immunofluorescent studies for GFAP plus collagen IV and α-SMA plus c-Met or GFRα-1 were also performed; c-Met is an HGF receptor and GFRα-1 is the most effective receptor for GDNF (Arvidsson et al., 2001). The staining steps were the same as in our previous report (Deguchi et al., 2006). Each dilution of the first antibody was as follows: biotinylated LEL (Vector) at 1:200, rabbit polyclonal anti-GFAP antibody (Dako, Carpinteria, CA) at 1:1,000, goat polyclonal anti-DCX antibody (Santa Cruz Biotechnology, Santa Cruz, CA) at 1:200, mouse monoclonal anti-BrdU antibody (Oncogene Research Products) at 1:200, mouse monoclonal anti-type IV collagen antibody (Abcam, Cambridge, MA) at 1:100, mouse monoclonal anti-α-SMA (Sigma) at 1:200, rabbit anti-GFRα-1 (Sigma) at 1:500, and rabbit monoclonal anti-c-Met (Abcam) at 1:200. The second antibody was Texas red-labled anti-mouse IgG antibody (Vector) at 1:200 simultaneously with FITC avidin D (Vector) or FITC-labled secondary antibodies (Vector). The slides were covered with Vectashield mounting medium with 4′,6′-diamidino-2-phenylindole (Vector). The treated sections were scanned with a confocal microscope equipped with an argon and HeNe1 laser (LSM-510; Zeiss, Jena, Germany). Sets of fluorescent images were acquired sequentially for the red and green channels to prevent crossover of signals from green to red or from red to green channels.

Quantitative Analysis

To evaluate the results of TUNEL staining analysis quantitatively, the positively stained cells were counted in the cerebral cortex and dorsal caudate of the MCA territory in five coronal sections per rat brain. To evaluate the results of neurogenesis and synaptogenesis, the positively stained cells were counted for BrdU, DCX/BrdU, and GFAP/BrdU in the subventricular zone (SVZ), GAP-43 in the periinfarct region in five coronal sections per rat brain. To evaluate the angiogenesis result, the positively stained cells were counted for NAGO/BrdU in the ischemia boundary zone in five coronal sections per rat brain. For the semiquantitative evaluation of staining, blood vessels and cells were identified by their morphology, and the staining intensity was measured in Scion Image. NAGO was evaluated in the periinfarct zone; collagen IV and GFAP were evaluated in the overlapping zone of collagen IV and GFAP-positive areas in five coronal sections per rat brain as in our previous report (Yamashita et al., 2009a).

Statistical Analysis

All data are expressed as mean ± SD. The one-way ANOVA and Fisher's PLSD post hoc test were used for each evaluation.

RESULTS

Quantitative Analysis of Infarct Volume

HE staining showed that 90 min of MCAO caused large infarcts of the lateral cortex and the underlying caudoputamen. Infarct areas of five coronal sections (2, 4, 6, 8, and 10 mm caudal from frontal pole) are shown in Figure 1a. The infarct volume of the vehicle-treated group was 436.0 ± 30.9 mm^3 (mean ± SD), GDNF-treated group 226.0 ± 42.6 mm^3, and HGF-treated group 306.0 ± 33.1 mm^3. The infarct volume of HGF ($*P < 0.05$)- and GDNF ($**P < 0.01$)-treated groups was significantly smaller than that of vehicle-treated group, and GDNF significantly decreased the infarct volume than HGF ($*P < 0.05$; Fig. 1b).

Antiapoptotic Effect

The TUNEL-positive stained cells were distributed in the cerebral cortex and dorsal caudate of the MCA territory but were not found in other areas of the ipsilateral hemisphere or the contralateral side (Fig. 1c). The staining was found exclusively in the nuclei of neuronal cells. A strong staining for TUNEL was present in the vehicle-treated group, but the treatment with HGF and GDNF significantly reduced the number of TUNEL-positive cells on day 14 after tMCAO, and GDNF significantly decreased the number of TUNEL-positive cells more than HGF [$*P < 0.05$): 352.2 ± 59.2/mm^2 (mean ± SD) in the vehicle-treated group, 199.9 ± 48.6/mm^2 ($*P < 0.05$) in HGF-treated group, and 98.6 ± 38.5/mm^2 ($**P < 0.01$) in GDNF-treated group; Fig. 1d].

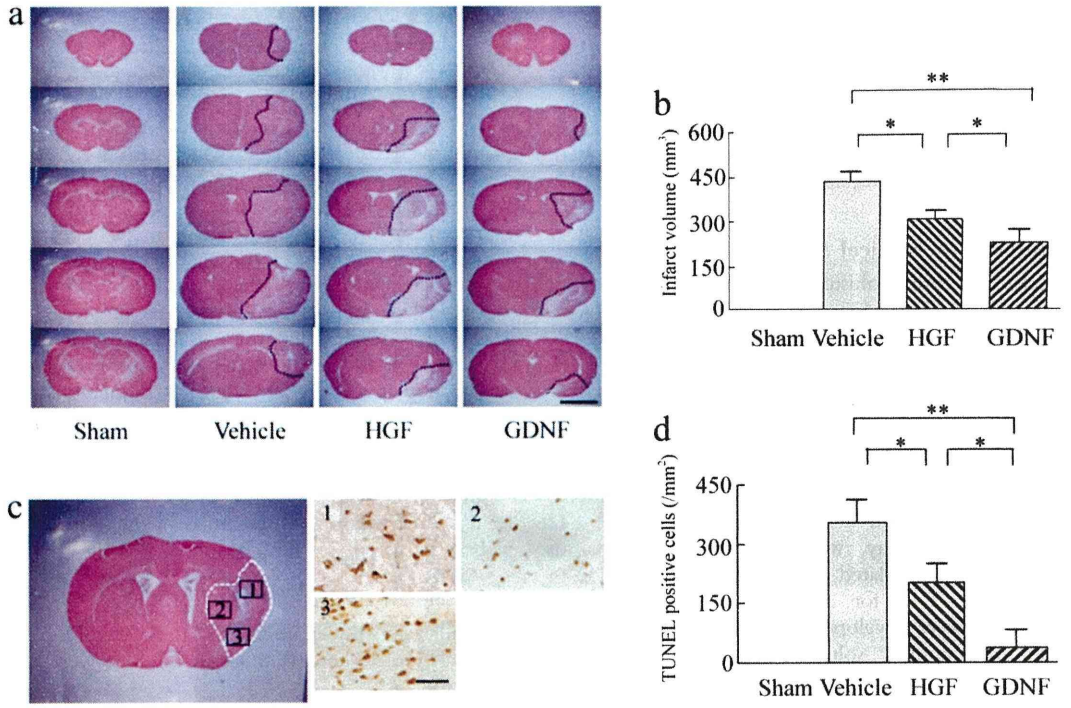

Fig. 1. Infarct volume change and evaluation of the antiapoptotic effect on day 14 after tMCAO. HE staining (**a**) and quantitative analysis of infarct volume (**b**). TUNEL staining (**c**) and quantitative analysis of TUNEL-positive cells (**d**). $*P < 0.05$, $**P < 0.01$. Scale bars = 5 mm in a; 70 μm in c.

Cell Proliferation in the SVZ

BrdU-positive cells were detected in the SVZ in normal brain, the number of which markedly increased in SVZ after tMCAO (vehicle, 159.5 ± 42.7/mm^2). Treatment with HGF (339.2 ± 53.7/mm^2) greatly enhanced the number of such BrdU-positive cells over vehicle, but not in the GDNF (178.8 ± 31.5/mm^2)-treated group (Fig. 2a,b).

Neurogenesis in the SVZ

DCX is a microtubule-associated protein, which is a marker of migratory or immature neurons. BrdU/DCX double-positive cells were detected in small numbers in SVZ of normal brain and were markedly increased after tMCAO (vehicle, 88.1 ± 16.3/mm^2). Treatment with HGF (266.9 ± 56.3/mm^2) greatly enhanced the number of BrdU/DCX double-positive cells over vehicle, but not in the GDNF (104.7 ± 38.6/mm^2)-treated group (Fig. 2c,d). Immunofluorescence double labeling for BrdU/GFAP was performed to follow mature astrocyte differentiation from newly proliferated cells in SVZ; the numbers of BrdU/GFAP double-positive cells were significantly increased in the HGF (190.3 ± 36.9/mm^2)-treated group over the vehicle (55.1 ± 14.4/mm^2) and GDNF (69.2 ± 28.4/mm^2)-treated groups (Fig. 2e,f).

Angiogenesis in the Cerebral Ischemic Boundary Zone

NAGO is a marker of the vascular endothelium. Angiogenesis occurred following cerebral ischemia; newly born vascular endothelial cells that were double-positive for BrdU/NAGO were clearly observed in the cerebral ischemic boundary zone, but not in the ischemic core (Fig. 2g). The number of BrdU/NAGO double-positive cells was significantly increased in the HGF-treated group over the vehicle ($**P < 0.01$) and GDNF ($**P < 0.01$)-treated groups (Fig. 2h). There was no difference between vehicle- and GDNF-treated groups. Administration of HGF also significantly increased vascular pixel intensity compared with the vehicle ($**P < 0.01$) and GDNF ($*P < 0.05$) groups on day 14 after tMCAO (Fig. 2i).

Synaptogenesis in the Cerebral Ischemic Boundary Zone

GAP-43 is considered a crucial component of the axon and presynaptic terminal and is recognized as a synaptic remodeling marker. The number of GAP-43-positive cells was markedly increased on day 14 after tMCAO in the cerebral ischemic boundary zone (vehicle, 59.8 ± 13.8/mm^2). Treatment with

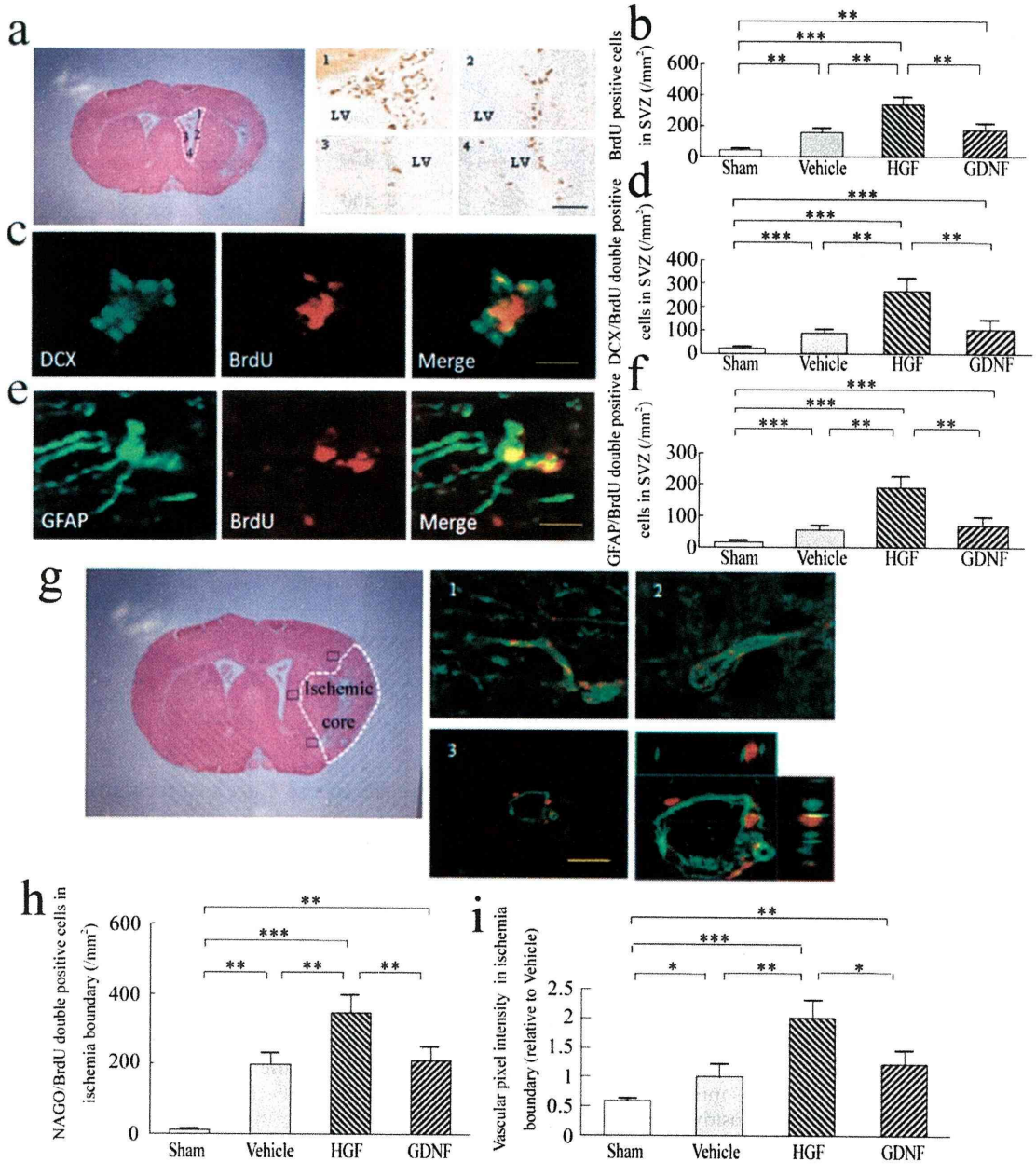

Fig. 2. Evaluating neurogenesis and angiogenesis on day 14 after tMCAO. BrdU immunohistochemical staining in SVZ (**a**) and quantitative analysis of BrdU-positive cells (**b**). Photomicrographs of DCX/BrdU double staining (**c**), GFAP/BrdU double staining (**e**) in the SVZ and NAGO/BrdU double staining (**g**) in the ischemia boundary. Quantitative analysis of DCX/double-positive cells (**d**), GFAP/BrdU double-positive cells (**f**), NAGO/BrdU double-positive cells (**h**), and vascular intensity (relative to vehicle; **i**). $*P < 0.05$, $**P < 0.01$, $***P < 0.001$. Scale bars = 70 μm in a; 20 μm in c,e.

HGF (95.4 ± 25.4/mm^2) significantly increased the number of GAP-43-positive cells compared with the vehicle- and GDNF (62.3 ± 16.9/mm^2)-treated groups (Fig. 3).

Antifibrosis After Cerebral Ischemia

Glial scar is formed via the accumulation of reactive astrocytes and is a major obstacle to axonal regener-

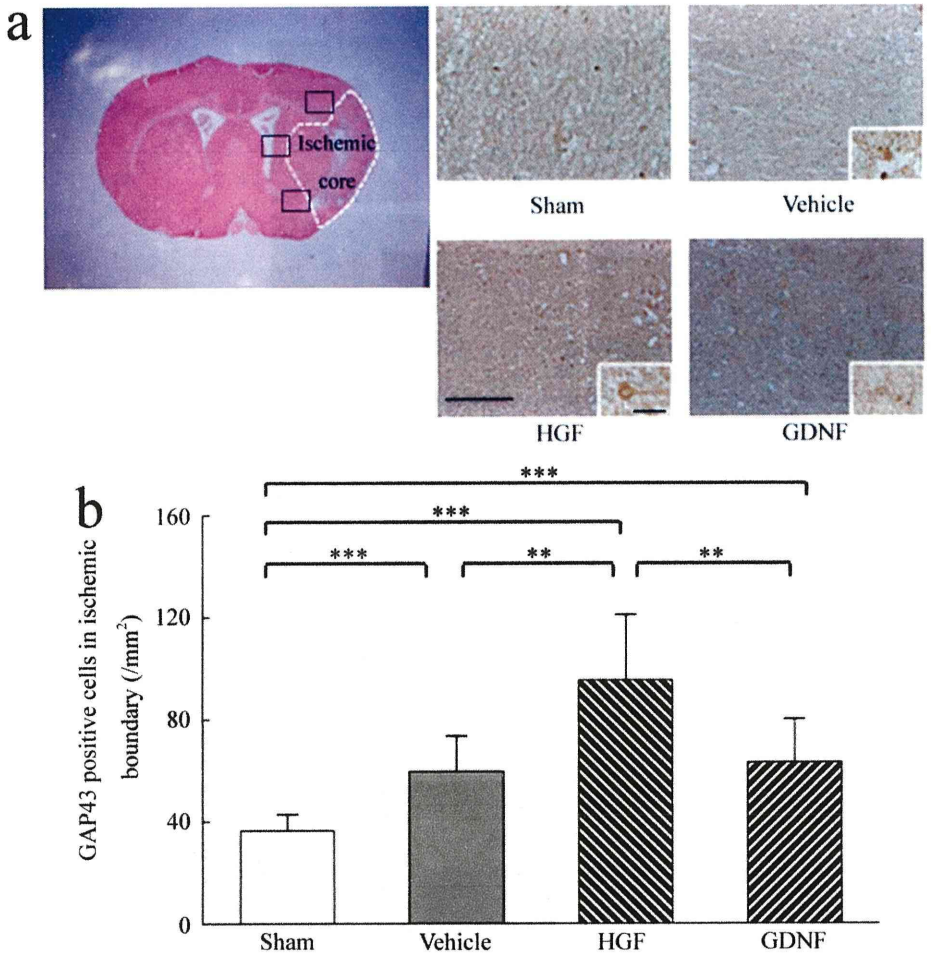

Fig. 3. Evaluating synaptogenesis on day 14 after tMCAO. Photomicrographs of GAP-43 immunostaining in the ischemia boundary (**a**) and quantitative analysis of GAP-43-positive cells (**b**). $^{**}P < 0.01$, $^{***}P < 0.001$. Scale bars = 100 μm in a; 70 μm in inset.

ation by neurons (Zhang et al., 2006). Immunofluorescence analysis showed that both GFAP and collagen IV expression became apparent 14 days after tMCAO (Fig. 4a). Collagen IV and GFAP pixel intensity were evaluated in the overlapping zone of positive areas (Fig. 4b). Administration of HGF significantly decreased collagen IV and GFAP pixel intensity compared with the vehicle and GDNF groups on day 14 after tMCAO. There was no difference between vehicle- and GDNF-treated groups (Fig. 4c,d). Pia mater was very thin in the normal animal (Fig. 4e; 6.7 ± 0.9 μm), but the pia mater became a scar at the contact interface of the brain and the spongel 14 days after the operation (vehicle, 26.3 ± 4.9 μm). The thickness of the scar stained by α-SMA was significantly decreased in the HGF-treated group (13.0 ± 3.4 μm) but not in the GDNF-treated group (25.9 ± 4.3 μm; Fig. 4e). Double-immunofluorescent studies for α-SMA plus c-Met (HGF receptor) or GFRα-1 (GDNF receptor) showed that the scar thickness was clearly reduced in the HGF-treated group (Fig. 4f). A summary for the pia mater thickness is shown in Figure 4g.

DISCUSSION

It has been reported that HGF specifically binds and activates a tyrosine kinase receptor encoded by the c-Met protooncogene (Bottaro et al., 1991); both HGF and c-Met were expressed in adult and fetal central nervous system (Maina and Klein, 1999). HGF activates c-MET and subsequent downstream pathways, including the antiapoptotic protein kinase-B (PKB/Akt) cascade, the proliferative MAP-kinase pathway (ERK1/2 and p38MAPK), and the STAT3 signaling (signal transducers and activators of transcription; Birchmeier et al., 2003). GDNF signals via multicomponent receptors consisting

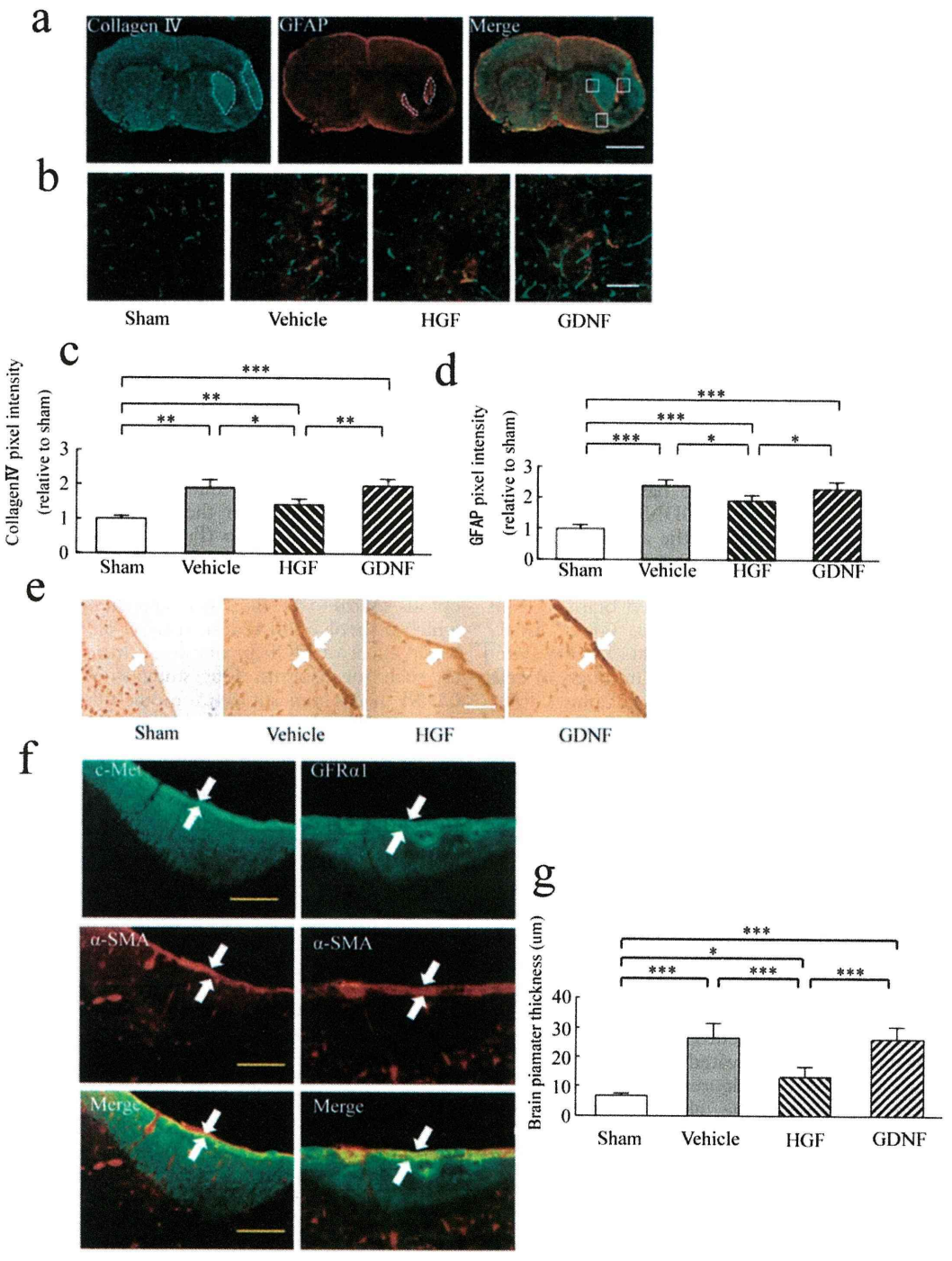

Fig. 4. Evaluating antifibrosis on day 14 after tMCAO. Double staining of GFAP and collagen IV in ischemic brain (**a**). Photomicrographs of collagen IV and GFAP in the overlapping zone of the positive areas (**b**). Quantitative analysis of collagen IV and GFAP pixel intensity in the overlapping zone of the positive areas (**c,d**). Photomicrographs of α-SMA immunostaining (**e**) and c-Met (HGF receptor) or GFRα-1 (GDNF receptor) plus α-SMA double staining (**f**) and quantitative analysis of the scar at the contact interface of the ischemic brain and spongel on day 14 after tMCAO (**g**). $*P < 0.05$, $**P < 0.01$, $***P < 0.001$. Scale bars = 5 mm in a; 50 μm in b,e,f.

of the Ret receptor tyrosine kinase plus a glycosylphosphatidylinositol-linked coreceptor termed *GDNF family receptor-α1* (GFRα1). After binding to its specific receptor complex, GDNF activates several downstream intracellular pathways, including phosphatidylinositol 3-kinase/protein kinase B (PI3K/Akt; Soler et al., 1999) and extracellular signal-regulated kinase 1/2/mitogen-activated protein kinase (ERK1/2 MAPK) pathways (Worby et al., 1996). Signals through PI3K/Akt or ERK1/2MAPK pathways lead to different trophic effects. The most widespread paradigm is that the PI3K/Akt pathway is involved in cellular survival (Hetman et al., 1999), whereas the ERK1/2 MAPK pathway is involved in neuronal differentiation (Perron and Bixby, 1999), and phosphorylation of Akt and ERK promotes synaptic plasticity (Daw et al., 2002). Similarly, activation of the PI3 kinase/Akt pathway, which is a well-known way to inhibit apoptosis, also inhibits autophagy (Arico et al., 2001). Our results show that postischemic administration of HGF and GDNF in the acute phase significantly reduced infarct size and the number of TUNEL-positive cells (Fig. 1). We have reported that the protective effects of HGF and GDNF in acute phase of stroke are highly associated with the antiapoptotic and antiautophagic effects (Shang et al., 2010).

To evaluate potential effects of HGF and GDNF in the chronic phase of stroke, we probed brain sections with BrdU, BrdU plus DCX, BrdU plus GFAP, BrdU plus NAGO, and GAP-43 antibody at 14 day after tMCAO (Figs. 2, 3). We found that the numbers of cells positive for BrdU, BrdU plus DCX, BrdU plus GFAP, GAP-43, BrdU plus NAGO and vascular pixel intensity were significantly increased after tMCAO. Those changes were greatly enhanced in HGF-treated group, while not in GDNF-treated group. Our results suggest that ischemic stroke induced neurogenesis, angiogenesis, and synaptogenesis that were in accordance with previous reports (Jin et al., 2001; Beck and Plate, 2009; Jung et al., 2009). However, we first showed that such neurogenesis, angiogenesis, and synaptogenesis were greatly amplified by HGF treatment. Although Kobayashi et al. (2006) reported that intracerebral infusion of GDNF promoted striatal neurogenesis after stroke in adult rats, our present study shows that there were no significant differences of angiogenesis, neurogenesis, and synaptogenesis between the GDNF-treated group and the vehicle-treated group. The possible reasons why HGF was stronger than GDNF in the above-described triple genetic effects may be as follows. 1) HGF activates more direct downstream intracellular pathways than GDNF for cell proliferation and differentiation. For example, HGF activates STAT translocation from cytoplasm to the nucleus and regulates specific target gene expression, which allows cell proliferation and differentiation (Shuai et al., 1993). 2) The effects of HGF are mediated via activation of vascular endothelial growth factor (VEGF; Van Belle et al., 1998), which promotes a strong angiogenesis (Leung et al., 1989), stimulates a neurogenesis in vitro and in vivo (Jin et al., 2002), and stimulates axon outgrowth (Sondell et al., 2000). In fact, HGF promoted axonal growth of dorsal root ganglion (DRG) sensory neurons in cooperation with nerve growth factor (NGF; Maina et al., 1997).

To evaluate antifibrotic effects of HGF and GDNF, we probed brain sections with collagen IV and GFAP at 14 days after tMCAO (Fig. 4a,b). Collagen IV is an important marker for glial scar, appearing at late stages of glial scar (Liesi and Kauppila, 2002). Our results showed that administration of HGF significantly decreased collagen IV and GFAP pixel intensity compared with the vehicle and GDNF groups 14 days after tMCAO (Fig. 4c,d). α-SMA is an actin isoform that contributes to cell-generated mechanical tension. α-SMA is normally located only in vascular smooth muscle cells, but it can also be expressed in certain nonmuscle cells. Thus expression of α-SMA is considered to be a useful phenotypic marker for myofibroblasts (Tomasek et al., 2002). We first probed brain pia mater with an α-SMA antibody (Fig. 4e,f) and found that the brain pia mater had developed a scar at the contact interface of the ischemic brain and the spongel at day 14 after tMCAO (Fig. 4e). The thickness of the scar was significantly decreased only in the HGF-treated group, not in the GDNF-treated group (Fig. 4g). Recent studies suggest that HGF also has an antifibrotic effect through possible mechanisms such as a key ligand to elicit myofibroblast apoptosis (Mizuno et al., 2005) and an inhibition of ACE, which is involved in fibrosis (Day et al., 2003). The antifibrotic effect of HGF in our study may also be dependent on such mechanisms. Our study shows both HGF and GDNF had significant neurotrophic effects, but they have different effects after cerebral ischemia. In summary, our present data showed both HGF and GDNF had neurotrophic effects. However, only HGF, and not GDNF, showed angiogenetic, neurogenetic, and synaptogenetic effects in brains after tMCAO. Furthermore, HGF decreased the glial scar formation and the scar thickness of the brain pia mater after tMCAO. HGF should be a better choice as a reagent that has a wide variety of mechanisms and a long-lasting effect in future human stroke, when both multiple steps of injury and molecular processes of recovery are dramatically and time dependently changing.

ACKNOWLEDGMENTS

We thank Kringle Pharma (Osaka, Japan) for the gift of HGF. The authors declare that they have no competing financial interests.

REFERENCES

Abe K. 2000. Therapeutic potential of neurotrophic factors and neural stem cells against ischemic brain injury. J Cereb Blood Flow Metab 20:1393–1408.

Abe K, Kawagoe J, Araki T, Aoki M, Kogure K. 1992. Differential expression of heat shock protein 70 gene between the cortex and caudate after transient focal cerebral ischemia in rats. Neurol Res. 14:381–385.

Abe K, Hayashi T, Itoyama Y. 1997. Amelioration of brain edema by topical application of glial cell line-derived neurotrophic factor in reperfused rat brain. Neurosci Lett 231:37–40.

Arico S, Petiot A, Bauvy C. 2001. The tumor suppressor PTEN positively regulates macroautophagy by inhibiting the phosphatidylinositol 3-kinase/protein kinase B pathway. J Biol Chem 276:35243–35246.

Arvidsson A, Kokaia Z, Airaksinen MS, Saarma M, Lindvall O. 2001. Stroke induces widespread changes of gene expression for glial cell line-derived neurotrophic factor family receptors in the adult rat brain. Neuroscience 106:27–41.

Augustin HG, Braun K, Telemenakis I, Modlich U, Kuhn W. 1995. Ovarian angiogenesis. Phenotypic characterization of endothelial cells in a physiological model of blood vessel growth and regression. Am J Pathol 147:339–351.

Beck H, Plate KH. 2009. Angiogenesis after cerebral ischemia. Acta Neuropathol 117:481–496.

Beck KD, Valverde J, Alexi T, Poulsen K, Moffat B, Vandlen RA, Rosenthal A, Hefti F. 1995. Mesencephalic dopaminergic neurons protected by GDNF from axotomy-induced degeneration in the adult brain. Nature 373:339–341.

Birchmeier C, Birchmeier W, Gherardi E, Vande Woude GF. 2003. Met, metastasis, motility and more. Nat Rev Mol Cell Biol 4:915–925.

Bottaro DP, Rubin JS, Faletto DL, Chan A M, Kmiecik TE, Vande Woude GF, Aaronson SA. 1991. Identification of the hepatocyte growth factor receptor as the c-Met proto-oncogene product. Science 251:802–804.

Chen J, Chopp M. 2006. Neurorestorative treatment of stroke: cell and pharmacological approaches. NeuroRx 3:466–473.

Daw MI, Bortolotto ZA, Saulle E. 2002. Phosphatidylinositol 3 kinase regulates synapse specificity of hippocampal long-term depression. Nat Neurosci 5:835–836.

Day RM, Thiel G, Lum J, Chévere RD, Yang Y, Stevens J, Sibert L, Fanburg BL. 2003. Hepatocyte growth factor regulates angiotensin converting enzyme expression. J Biol Chem 279:8792–8801.

Deguchi K, Tsuru K, Hayashi T, Takaishi M, Nagahara M, Nagotani S, Sehara Y, Jin G, Zhang H, Huh NH, Abe K. 2006. Implantation of a new porous gelatin-siloxane hybrid into a brain lesion as a potential scaffold for tissue regeneration. J Cereb Blood Flow Metab 26:1263–1273.

Folkman J, Shing Y. 1992. Angiogenesis. J Biol Chem 267:10931–10934.

Hetman M, Kanning K, Cavanaugh JE, Xia Z. 1999. Neuroprotection by brainderived neurotrophic factor is mediated by extracellular signal-regulated kinase and phosphatidylinositol 3-kinase. J Biol Chem 274:22569–22580.

Jin K, Minami M, Lan JQ, Mao XO, Batteur S, Simon RP, Greenberg DA. 2001. Neurogenesis in dentate subgranular zone and rostral subventricular zone after focal cerebral ischemia in the rat. Proc Natl Acad Sci U S A 98:4710–4715.

Jin K, Zhu Y, Sun Y, Mao XO, Xie L, Greenberg DA. 2002. Vascular endothelial growth factor (VEGF) stimulates neurogenesis in vitro and in vivo. Proc Natl Acad Sci U S A 99:11946–11950.

Jung SH, Lee ST, Chu K, Park JE, Lee SU, Han TR, Kim M. 2009. Cell proliferation and synaptogenesis in the cerebellum after focal cerebral ischemia. Brain Res 1284:180–190.

Kernie SG, Parent JM. 2009. Forebrain neurogenesis after focal Ischemic and traumatic brain injury. Neurobiol Dis 37:267–274.

Kobayashi T, Ahlenius H, Thored P, Kobayashi R, Kokaia Z, Lindvall O. 2006. Intracerebral infusion of glial cell line-derived neurotrophic factor promotes striatal neurogenesis after stroke in adult rats. Stroke 37:2361–2367.

Koizumi J, Yoshida Y, Nakazawa T. 1986. Experimental studies of ischemic brain edema: a new experimental model of cerebral embolism in rats in which recirculation can be induced in the ischemic area. Jpn J Stroke 8:1–7.

Lee SH, Kim YJ, Lee KM, Ryu S, Yoon BW. 2007. Ischemic preconditioning enhances neurogenesis in the subventricular zone. Neuroscience 146:1020–1031.

Leung DW, Cachianes G, Kuang WJ, Goeddel DV, Ferrara N. 1989. Vascular endothelial growth factor is a secreted angiogenic mitogen. Science 246:1306–1309.

Liesi P, Kauppila T. 2002. Induction of type IV collagen and other basementmembrane-associated proteins after spinal cord injury of the adult rat may participate in formation of the glial scar. Exp Neurol 173:31–45.

Maina F, Klein R. 1999. Hepatocyte growth factor, a versatile signal for developing neurons. Nat Neurosci 2:213–217.

Maina F, Hilton MC, Ponzetto C, Davies AM, Klein R. 1997. Met receptor signaling is required for sensory nerve development and HGF promotes axonal growth and survival of sensory neurons. Genes Dev 11:3341–3350.

Matsumoto K, Nakamura T. 1996. Emerging multipotent aspects of hepatocyte growth factor. J Biochem 119:591–600.

Miyazawa T, Matsumoto K, Ohmichi H, Katoh H, Yamashima T, Nakamura T. 1998. Protection of hippocampal neurons from ischemia-induced delayed neuronal death by hepatocyte growth factor: a novel neurotrophic factor. J Cereb Blood Flow Metab 18:345–348.

Mizuno S, Matsumoto K, Li MY, Nakamura T. 2005. HGF reduces advancing lung fibrosis in mice: a potential role for MMP-dependent myofibroblast apoptosis. FASEB J 19:580–582.

Nakamura T, Nishizawa T, Hagiya M, Seki T, Shimonishi M, Sugimura A, Tashiro K, Shimizu S. 1989. Molecular cloning and expression of human hepatocyte growth factor. Nature 342:440–443.

Niimura M, Takagi N, Takagi K, Funakoshi H, Nakamura T, Takeo S. 2006. Effects of hepatocyte growth factor on phosphorylation of extracellular signal-regulated kinase and hippocampal cell death in rats with transient forebrain ischemia. Eur J Pharmacol 535:114–124.

Nudo RJ. 2003. Functional and structural plasticity in motor cortex: implications for stroke recovery. Phys Med Rehabil Clin North Am 14(Suppl 1):S57–S76.

Oestreicher AB, De Graan PN, Gispen WH, Verhaagen J, Schrama LH. 1997. B-50, the growth associated protein-43: modulation of cell morphology and communication in the nervous system. Prog Neurobiol 53:627–686.

Otto D, Frotscher M, Uniscker K. 1989. Basic fibroblast growth factor and nerve growth factor administrated in gel foam rescue medial septal neurons after fimbria fornix transection. J Neurosci Res 22:83–91.

Perron JC, Bixby JL. 1999. Distinct neurite outgrowth signaling pathways converge on ERK activation. Mol Cell Neurosci 13:362–378.

Shang J, Deguchi K, Yamashita T, Matsuura T, Funakoshi H, Nakamura T, Abe K. 2010. Antiapoptotic and antiautophagic effects of glial cell line-derived neurotrophic factor and hepatocyte growth factor after transient middle cerebral artery occlusion in rats. J Neurosci Res 88:2197–2206.

Shuai K, Ziemiecki A, Wilks AF, Harpur AG, Sadowski HB, Gilman MZ, Darnell JE. 1993. Polypeptide signalling to the nucleus through tyrosine phosphorylation of Jak and Stat proteins. Nature 366:580–583.

Soler RM, Dolcet X, Encinas M, Egea J, Bayascas JR, Comella JX. 1999. Receptors of the glial cell line-derived neurotrophic factor family of neurotrophic factors signal cell survival through the phosphatidylinositol 3-kinase pathway in spinal cord motoneurons. J Neurosci 19:9160–9169.

Sondell M, Sundler F, Kanje M. 2000. Vascular endothelial growth factor is a neurotrophic factor which stimulates axonal outgrowth through the flk-1 receptor. Eur J Neurosci 12:4243–4254.

Tomasek JJ, Gabbiani G, Hinz B, Chaponnier C, Brown RA. 2002. Myofibroblasts and mechano-regulation of connective tissue remodelling. Nat Rev Mol Cell Biol 3:349–363.

Van Belle E, Witzenbichler B, Chen D, Silver M, Chang L, Schwall R, Isner JM. 1998. Potentiated angiogenic effect of scatter factor/hepatocyte growth factor via induction of vascular endothelial growth factor: the case for paracrine amplification of angiogenesis. Circulation 97:381–390.

Worby CA, Vega QC, Zhao Y, Chao HH, Seasholtz AF, Dixon JE. 1996. Glial cell line-derived neurotrophic factor signals through the RET receptor and activates mitogen-activated protein kinase. J Biol Chem 271:23619–23622.

Yamashita T, Kamiya T, Deguchi K, Inaba T, Zhang H, Shang J, Miyazaki K, Ohtsuka A, Katayama Y, Abe K. 2009a. Dissociation and protection of the neurovascular unit after thrombolysis and reperfusion in ischemic rat brain. J Cereb Blood Flow Metab 29:715–725.

Yamashita T, Deguchi K, Nagotani S, Kamiya T, Abe K. 2009b. Gene and stem cell therapy in ischemic stroke. Cell Transplant 18:999–1002.

Zarnegar R, Michalopoulos GK. 1995. The many faces of hepatocyte growth factor: from hepatopoiesis to hematopoiesis. J Cell Biol 129:1177–1180.

Zhang H, Muramatsu T, Murase A, Yuasa S, Uchimura K, Kadomatsu K. 2006. N-Acetylglucosamine 6-O-sulfotransferase-1 is required for brain keratan sulfate biosynthesis and glial scar formation after brain injury. Glycobiology 16:702–710.

***** 事務局 *****
東北大学大学院医学系研究科神経内科
〒980-8574 仙台市青葉区星陵町1-1
担当 伊藤詩織
電話 022-717-7189 / Fax 022-717-7192